Modeling Vessel-Generated Currents in Inland Waterways

Richard L. Stockstill and R.C. Berger
U.S. Army Engineer Waterways Experiment Station

INTRODUCTION

The movement of a vessel along a waterway produces a local depression in the water surface as the flow accelerates around the vessel. These vessel-induced flows are termed "return currents." The depression around the vessel and the surge that propagates ahead of it permeate the surrounding secondary channel and backwater areas. This produces some flushing of the backwater areas and sometimes significant currents near their entrances. Knowing the magnitudes of drawdown, return currents, and flushing may be important in the environmental impact assessment. Pressure changes and shear stresses on the riverbed due to vessel passage may suspend sediments, which are then transported by the river's ambient current and the vessel-generated currents. Drawdown of the water surface in shallow regions can result in short-term drying of these areas. Successful sediment-transport modeling depends on accurate predictions of water velocity's magnitude and direction. The currents at backwater entrances are sometimes significant due to the initial drawdown and subsequent reflections.

Much research has been directed to describing vessel drawdown and return currents. Empirical and one-dimensional analytic descriptions of vessel drawdown and return currents have been developed for confined prismatic waterways (e.g., *1–6*). However, the drawdown and return currents in large shallow areas around the channel or in more general complex channels cannot be evaluated using these basic descriptions.

The objective of this work is to demonstrate a numerical model to quantify vessel-generated currents for general waterways. It addresses the drawdown and return currents generated by the displacement of a vessel moving relative to the water. It does not, however, include propeller-generated currents. Included in this paper are the governing equations and assumptions made in their derivation. Details of the numerical model and extensive model testing with laboratory data have been reported (*7*). However, applications to actual river reaches and flow conditions are given for the first time. Two pools, one on the upper Mississippi River and one on the Illinois Waterway, are modeled simulating barge trains and river conditions existing during field observations made by others.

GOVERNING EQUATIONS

In this work, a pressure field is used to produce the drawdown of a moving vessel. This moving pressure field then results in the drawdown and flow fields throughout the modeled waterway. The movement of the pressure field in time is specified to represent a vessel hull navigating along a channel. This system is mathematically described using two-dimensional (2D), unsteady depth-averaged equations. These shallow-water (or long-wave) equations are a result of the vertical integration of the equations of mass and momentum conservation for incompressible flow under the hydrostatic pressure assumption. This assumption implies that vertical accelerations are negligible when compared with the horizontal accelerations and the acceleration due to gravity. The vertical accelerations are small when the characteristic wavelength is long relative to the depth. The drawdown wave is on the order of the length of the barge train, which is much greater than the channel depth. The hydrostatic pressure assumption is not accurate in the immediate vicinity of the tow, because flow accelerations produced by the boat displacement include significant vertical accelerations. However, the shallow-water equations conserve horizontal momentum and so are appropriate descriptions in the far field.

The dependent variables of the fluid motion are defined by the flow depth *(h)*, the *x*-component of unit discharge (*p*), and the *y*-component of unit discharge (*q*). These dependent variables are functions of the two space directions (*x* and *y*) and time (*t*). If the fluid pressure at the surface is included while the free-surface stresses are neglected, the shallow water equations are given as (*8*):

$$\frac{\partial \boldsymbol{U}}{\partial t} + \frac{\partial \boldsymbol{F}}{\partial x} + \frac{\partial \boldsymbol{G}}{\partial y} + \boldsymbol{H} = \boldsymbol{0} \tag{1}$$

where:

$$\boldsymbol{U} = \begin{Bmatrix} h \\ p \\ q \end{Bmatrix} \tag{2}$$

$$\boldsymbol{F} = \begin{Bmatrix} p \\ \dfrac{p^2}{h} + \frac{1}{2}gh^2 - h\dfrac{\sigma_{xx}}{\rho} \\ \dfrac{pq}{h} - h\dfrac{\sigma_{yx}}{\rho} \end{Bmatrix} \tag{3}$$

$$\boldsymbol{G} = \begin{Bmatrix} q \\ \dfrac{pq}{h} - h\dfrac{\sigma_{xy}}{\rho} \\ \dfrac{q^2}{h} + \frac{1}{2}gh^2 - h\dfrac{\sigma_{yy}}{\rho} \end{Bmatrix} \tag{4}$$

and

$$\boldsymbol{H} = \begin{Bmatrix} 0 \\ gh\dfrac{\partial z_0}{\partial x} + \dfrac{h}{\rho}\dfrac{\partial P}{\partial x} + n^2 g\dfrac{p\sqrt{p^2 + q^2}}{h^{7/3}} \\ gh\dfrac{\partial z_0}{\partial y} + \dfrac{h}{\rho}\dfrac{\partial P}{\partial y} + n^2 g\dfrac{q\sqrt{p^2 + q^2}}{h^{7/3}} \end{Bmatrix} \tag{5}$$

Here, g is the acceleration due to gravity, XX is the fluid density, z_0 is the channel bed elevation, n is the Manning's roughness coefficient, and P is the pressure at the water surface. The σ's are the Reynolds stresses due to turbulence, where the first subscript indicates the direction, and the second indicates the face on which the stress acts. The pressure at the free surface is zero, and the pressure at the vessel location is related to the vessel draft as

$$\boldsymbol{P} = \rho g d \tag{6}$$

where d is the vessel draft. The pressure at the free surface is specified as zero throughout the flow field, with the exception of the area beneath the vessel where the pressure is given by the vessel's draft.

VESSEL REPRESENTATION

The coordinates of the vessel center ($\boldsymbol{S}$) are moved during each time step, in accordance with the vessel's sailing speed and direction, as:

$$\boldsymbol{S} = \boldsymbol{S}_0 + \Delta\boldsymbol{S} \tag{7}$$

where $\boldsymbol{S_0}$ is the initial location of the vessel corners, and $\Delta\boldsymbol{S}$ is computed as:

$$\Delta S = \begin{cases} \frac{1}{2} a t^2 & 0 \leq t \leq t_s \\ \frac{1}{2} a t_s^2 + a t_s (t - t_s) & t \geq t_s \end{cases} \tag{8}$$

where a is the specified vessel acceleration, t is the time, and t_s is the time at which the vessel reaches a constant velocity (at_s). Subsequent to determination of the vessel center location, the vessel corner coordinates are calculated from the vessel's length and width. The induced pressure field resulting from the vessel draft is applied to every node within the vessel boundary, as illustrated in Figure 1. The computational mesh is constructed such that pressure gradients are applied across the bow, stern, and each side boundary in a manner to maintain the appropriate blockage area (vessel submerged cross-sectional area).

NUMERICAL EXAMPLES

Tests were conducted to demonstrate the validity and limitations of this method. The applicability of the technique is demonstrated on the Kampsville site on the Illinois Waterway. The validity of the model in the far field was first tested. This site was used to make comparisons in an uncomplicated geometric setting for which there are physical model results as well as field data. The model was then applied to a very geometrically complex region of Pool 8 on the Mississippi River. The model results reveal regions subjected to the greatest vessel-induced effects.

Kampsville Site, Illinois Waterway

Numerical experiments were conducted to evaluate the 2D model's ability to simulate the currents and waves generated in the field by a vessel navigating along a waterway. The Kampsville site was chosen because prototype data are available for comparison. The Kampsville site is located on the Illinois Waterway system at RM 35.2. The field data sets used for the model evaluation were obtained by the Illinois State Water Survey (9). This study provides an excellent data set with which the numerical model can be evaluated.

The Kampsville site data set used for this study is for a 3-wide-by-4-long downbound barge train towed by the M.V. William C. Norman. The vessel, which traveled at 2.9 m/sec, was 237.7 m long by 32.0 m wide, and drafted at 2.74 m. The river flow rate was 628 m^3 /sec, with a 4.67 m depth at the thalwag. A sketch of the river cross section at Kampsville, on which the sailing line is referenced to the thalwag, is illustrated in Figure 2. The cross-section sketch also shows the location of the Illinois State Water Survey's gages. Details of the numerical model computational mesh in the vicinity of the data gages are illustrated in Figure 3. The reported model results are from nodes in the area where the mesh is refined. The selection of appropriate parameters for the model were made from hydraulic experience, and not as an adjustment to match the field results. The numerical model was run independently from the field testing, in a "blind" test.

Velocities are compared in the *x*-direction (parallel to path of tow) and in the *y*-direction (perpendicular to tow motion). Positive velocities in the *x*-direction are in the same direction as the tow motion. That is, return currents are taken as negative *x*-direction velocities. The *y*-direction velocities are positive in the direction away from the vessel. The timing scale is such that zero is the time when the bow reaches the probe river section.

Time series of computed velocities, compared with those measured in the field, are shown for the location of field gage 642 in Figure 4. Figure 5 summarizes the findings of these simulations. It illustrates the distribution of maximum return currents across the channel in comparison with field data (9) and a 1:25-scale physical model (10). The numerical model accurately reproduces the maximum return current at distances greater than about two vessel widths from the sailing line. Discrepancies in the immediate vicinity of the vessel result from the model's hydrostatic pressure assumption. Vessel movement generates significant vertical accelerations in and adjacent to the vessel path. However, horizontal momentum is conserved, and therefore, the model accurately simulates the far field, where the pressure distribution is hydrostatic.

Pool 8, Mississippi River

Model applications were made to Pool 8 on the upper Mississippi River. This river reach was selected because it is highly braided with many backwater areas, as shown on the computational mesh (Figure 6). The Pool 8 model reproduced more than 13 km of the Mississippi River, with the lower boundary just downstream of RM 689. The flow rate during the field testing period was 501 m^3 /sec. The vessel modeled, pushed by the M.V. Roy E. Claverie, was a downbound 3-wide- by-4-long barge train, drafted at 2.74 m, and traveled at an average speed of 3.15 m/sec. Further simulations, under a variety of conditions, were examined as a part of the overall study, though not reported here.

Figures 7a–d illustrate the temporal variations of currents attributed to the vessel, as measured in the field and computed. The longitudinal direction is the direction of the ambient current, and the lateral is perpendicular to the ambient current direction. Time-dependent vessel-generated currents at the points annotated on the computational mesh are shown in Figures 7a and 7b. These time series show the influence vessel passage has on the system in the backwater areas.

The moving vessel develops a drawdown that travels beside and with the vessel. This depression in the water surface then propagates into the backwaters and side channels, resulting in an exchange of volumes between the channel and these off-channel features. This vessel-generated water-surface depression will produce a drawdown at the inlet of a side channel or backwater, and a depression wave that travels through these channels at a celerity of roughly $(gh)_{1/2}$. Additional information as to how significant the vessel effects are in the backwater areas is provided in the plots on Figures 7c and 7d, where the velocity is the sum of the river flow and the vessel-generated currents. The model and field results showed similar vessel effects. In this case, the vessel impacts were not significant in the backwater areas.

Figures 8a and 8b show the maximum vessel-generated drawdown and currents, respectively, for this particular model simulation. In Figure 8a, the dark region delineates the areas for which the drawdown is greater than 0.1 m. The dark region of 8b indicates maximum vessel-generated currents greater than 0.2 m/sec. The larger drawdown occurs close to the channel and along nearby shorelines, as one would expect. The drawdown is also amplified in single inlet backwaters by reflection at the closed end. The larger vessel-generated currents also occurred near the channel and nearby shorelines, and are significant around the ends of islands and secondary channels. The velocities in the entrance to single inlet backwaters are also noteworthy. Entrances to secondary channels can have large currents not only due to the initial wave passage, but also due to subsequent reflections.

CONCLUSIONS

The 2D representation provides spatially varying information about the vessel-generated hydrodynamics in geometrically complex waterways and reproduces the temporal variations of vessel-passage events. The model is, however, limited to flows that are adequately described by the shallow-water equations. The method is valid in the far-field regions, where vertical accelerations are small. The model does not address short-wavelength phenomena such as bow and stern waves, nor does it attempt to reproduce the effects of a towboat's propeller jet.

Model comparison to field and physical model data for the Illinois Waterway, Kampsville site, demonstrates that the numerical model does effectively represent the vessel-generated currents in the far field (area greater than about two vessel-beam widths from the sailing line). Not only were the magnitudes accurately reproduced, but also the duration of the vessel-induced events was simulated. The Illinois Waterway has a relatively small cross section, and so the blockage area of the vessel is large. Vessel effects are more pronounced in waterways having relatively large blockage areas. The model was demonstrated on a complex waterway, Pool 8, Mississippi River. In this large pool, the vessel-generated effects were less, and while the model results compare well with field data, the impacts were often small.

Model results show that the most significant drawdowns occur near the channel and nearby shorelines, as one would expect, but also at the closed end of single-inlet backwaters, due to wave reflection. The vessel-generated currents are largest near the vessel but are significant at the entrances to secondary channels and backwaters. The current near the entrance to the secondary channels is due to the initial drawdown as well as subsequent reflections. The examples illustrate the difference in impacts on waterways such as the Illinois, as compared with the Upper Mississippi River. Contour drawings of the maximum vessel-generated drawdown and currents are useful in determining where vessel effects are significant. Perhaps even more important, these figures illustrate off-channel areas that are essentially oblivious to the vessel sailing in the main channel. The model can also serve as a useful tool in evaluating remediation plans.

ACKNOWLEDGMENT

The numerical experiments described and the results presented were obtained from research sponsored by the Upper Mississippi River-Illinois Waterway navigation study by the U.S. Army Engineer Waterways Experiment Station, Vicksburg, Miss. Permission was granted by the Chief of Engineers to publish this information.

REFERENCES

1. Maynord, S.T., and T.S. Siemsen. Return Velocities Induced by Shallow-Draft Navigation. *Proceedings of the 1991 National Conference on Hydraulic Engineering* (R.M. Shane, ed.), Nashville, Tennessee, ASCE, New York, Vol. 1, 1991, pp. 894–899.
2. Hochstein, A.B., and C.E. Adams. Influence of Vessel Movements on Stability of Restricted Channels. *Journal of Waterway, Port, Coastal, and Ocean Engineering*. ASCE, Vol. 115, No. 4, 1989, pp. 444–465.
3. Blaauw, H., and F. van der Knaap. Prediction of Squat of Ships Sailing in Restricted Water. *8th International Harbour Congress*, Antwerp, Belgium, 1983, pp. 2.81–2.93.
4. Simons, D.B., R.M. Li, Y.H. Chen, S.S. Ellis, and T.P. Chang. *Investigation of Effects of Navigation Traffic Activities on Hydrologic, Hydraulic, and Geomorphic Characteristics*. Report for the Environmental Work Team, Upper Mississippi River Commission Master Plan, Minneapolis, Minn., 1981.
5. Bouwmesster, J., E.J. van de Kaa, H.A. Nuhoff, and R.G.J. Orden. *24th International Navigation Congress*, Leningrad, Russia, Permanent International Association of Navigation Congresses, Section 1, Subject 3, 1977, pp. 139–158 .
6. Jansen, P.Ph., and J.B. Schijf. *18th International Navigation Congress*. Permanent International Association of Navigation Congresses, Rome, Section 1, Communication 1, 1953, pp. 175–197.
7. Stockstill, R.L., S.K. Martin, and R.C. Berger. Hydrodynamic Model of Vessel-Generated Currents. *Regulated Rivers: Research and Management*, Vol. 11, 1995, pp. 211–225.
8. Abbott, M.B. *Computational Hydraulics: Elements of the Theory of Free Surface Flows*. Pitman Advanced Publishing Ltd., London, 1979.

9. Bhowmik, N.G., T.W. Soong, and R. Xia. *Physical Effects of Barge Tows on the Upper Mississippi River System: Analysis of Existing Data Collected by the Illinois Water Survey from the Kampsville Site on the Illinois River*. Progress Report No. 2, Illinois State Water Survey, Champaign, Ill., 1993.
10. Maynord, S.T., and S.K. Martin. *Interim Report for the Upper Mississippi River-Illinois Waterway System Navigation Study, Physical Forces Study, Kampsville, Illinois, Waterway*. ENV Report 3, U.S. Army Engineer Waterways Experiment Station, Vicksburg, Miss., 1997.

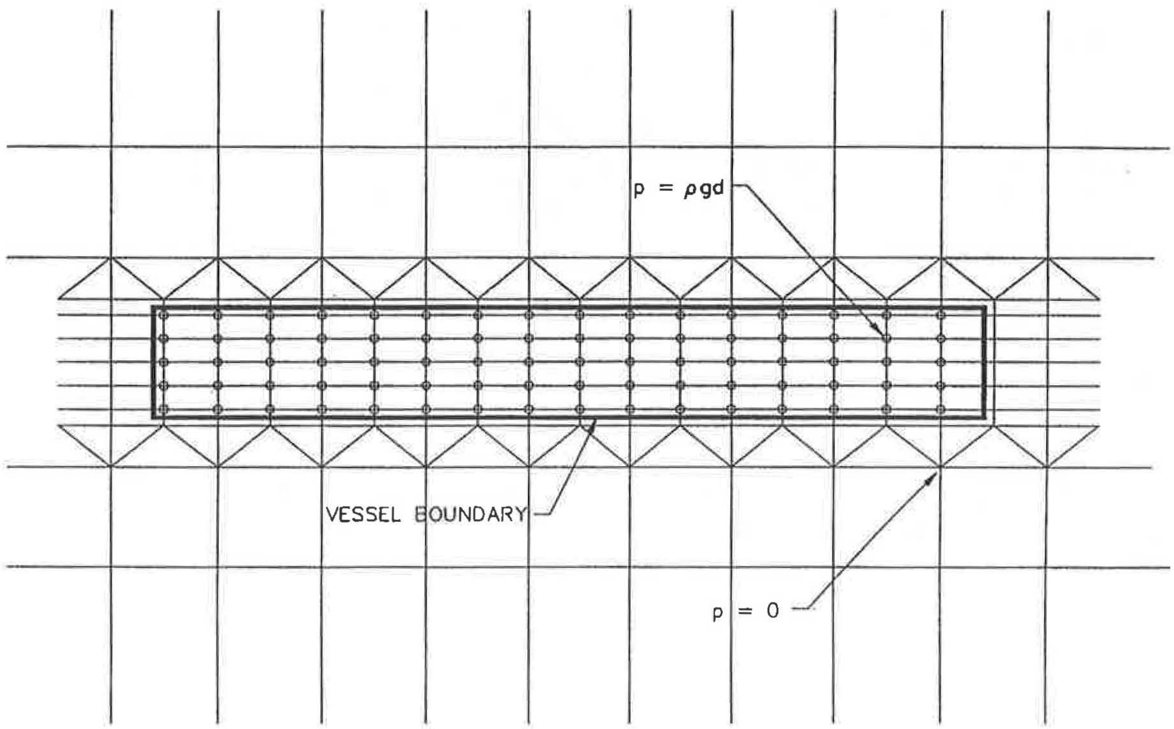

FIGURE 1 Discrete representation of a vessel on the numerical model computational mesh.

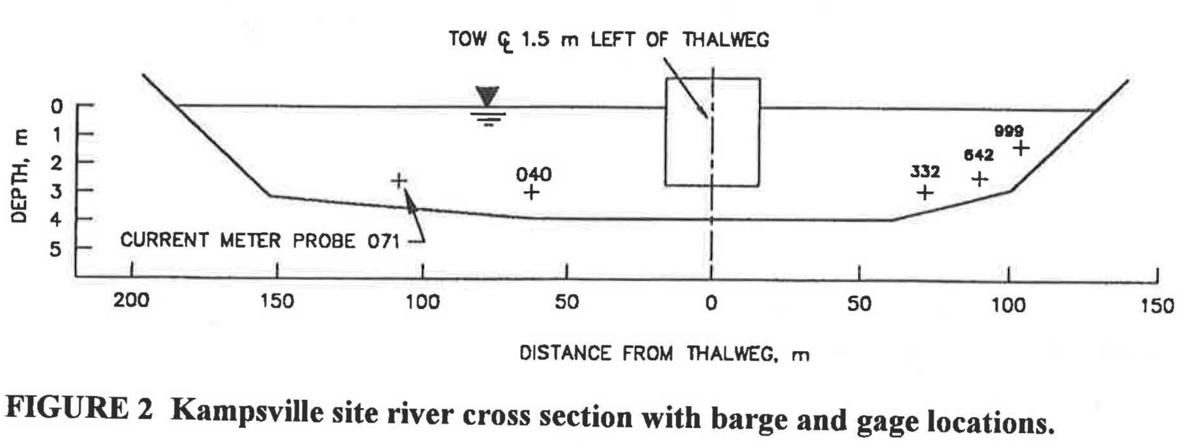

FIGURE 2 Kampsville site river cross section with barge and gage locations.

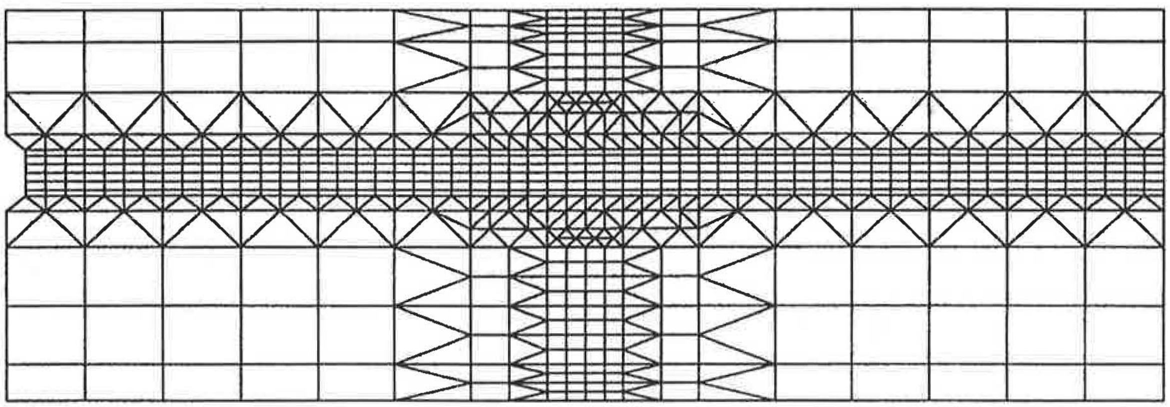

FIGURE 3 Numerical model computational mesh near the Kampsville site, Illinois Waterway (entire mesh had 2,069 nodes and 2,434 elements).

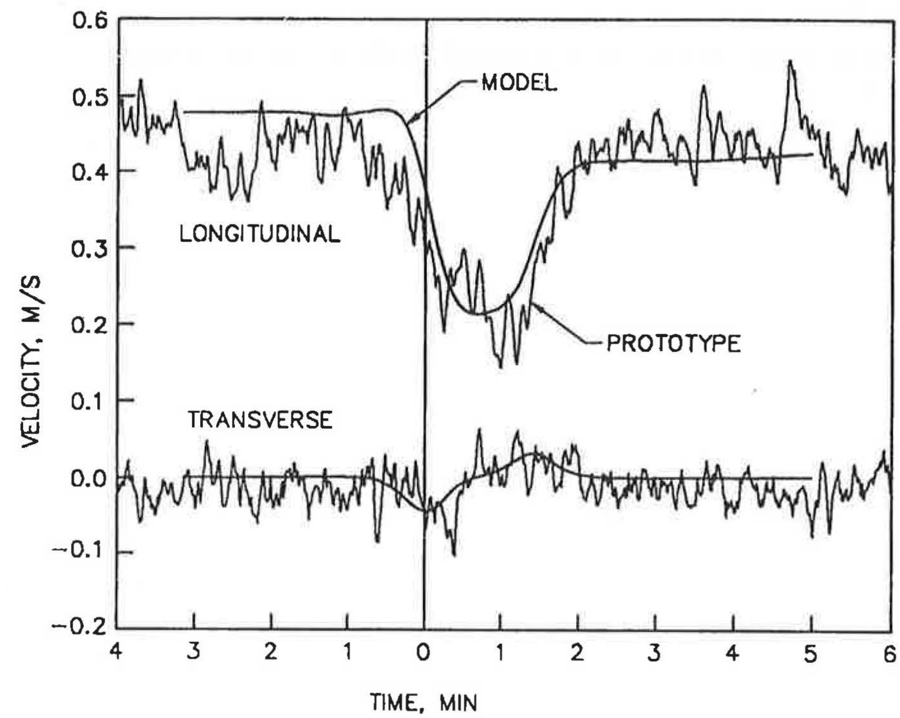

FIGURE 4 Computed and observed velocities at the Kampsville site, Illinois Waterway, field gage 642.

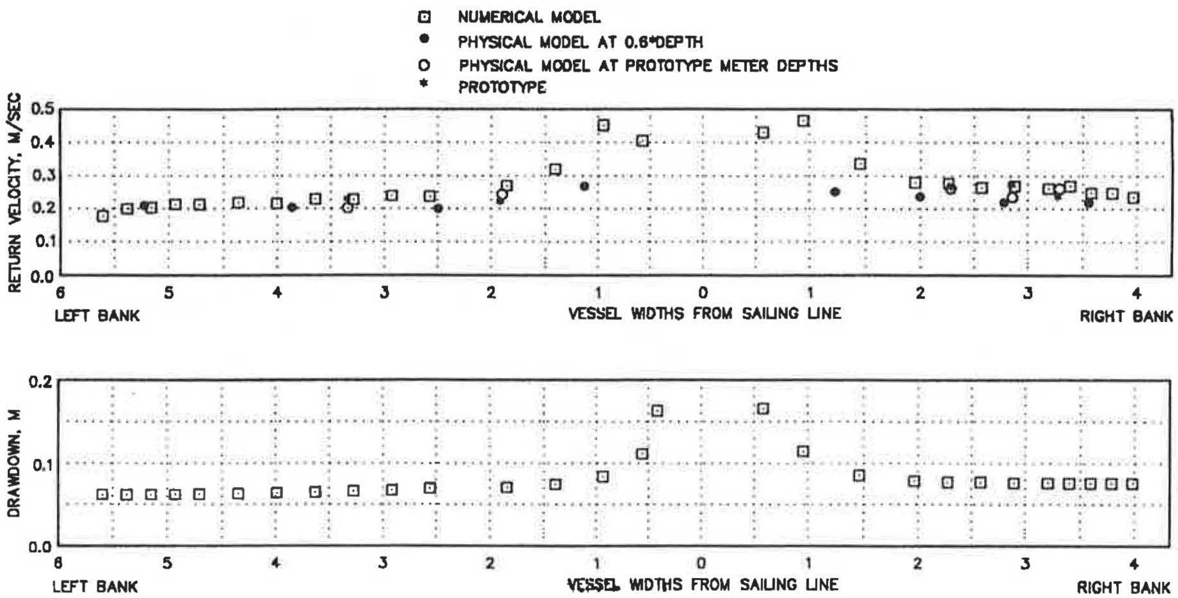

FIGURE 5 Return current and drawdown distribution at the Kampsville site.

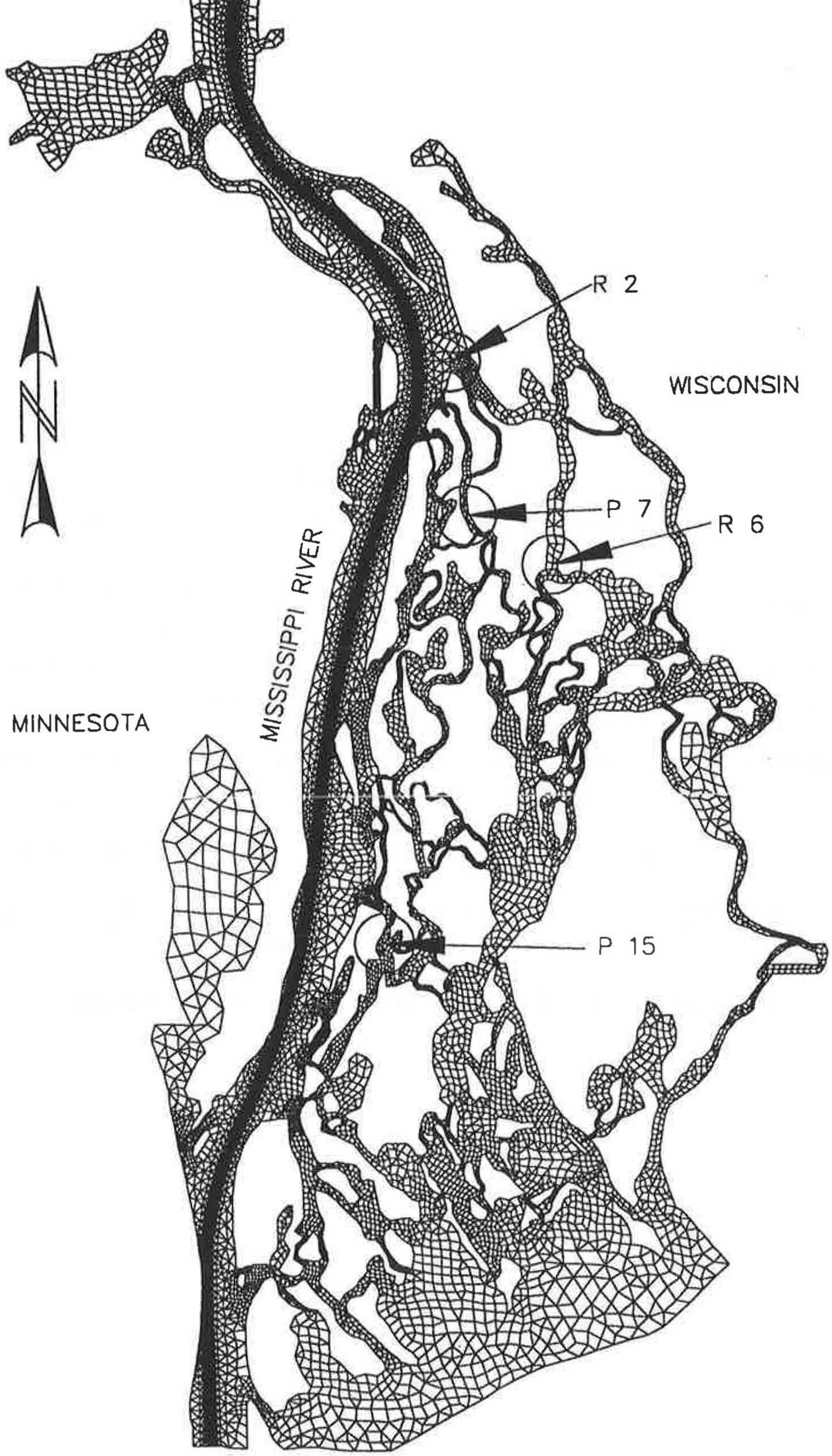

FIGURE 6 Pool 8, Mississippi River, numerical model computational mesh (16,198 nodes and 19,408 elements).

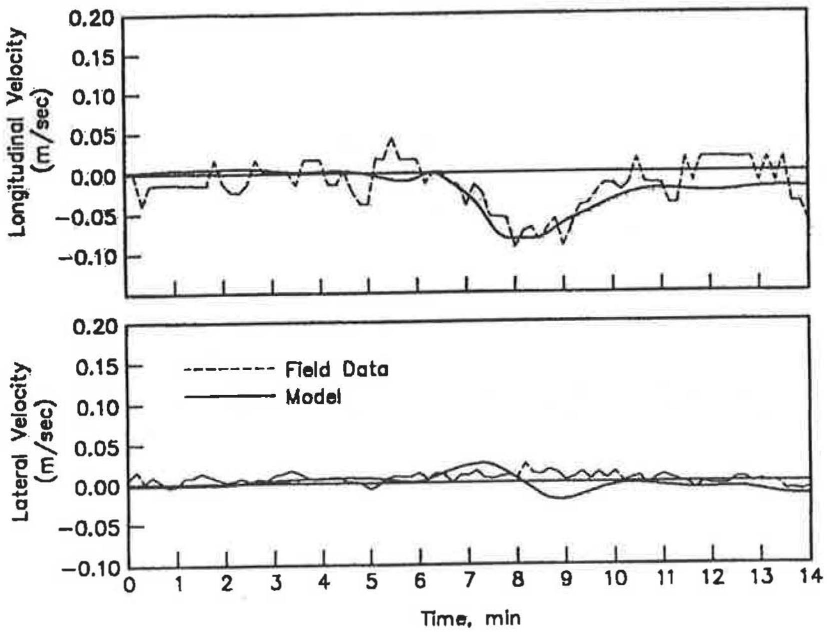

(a)

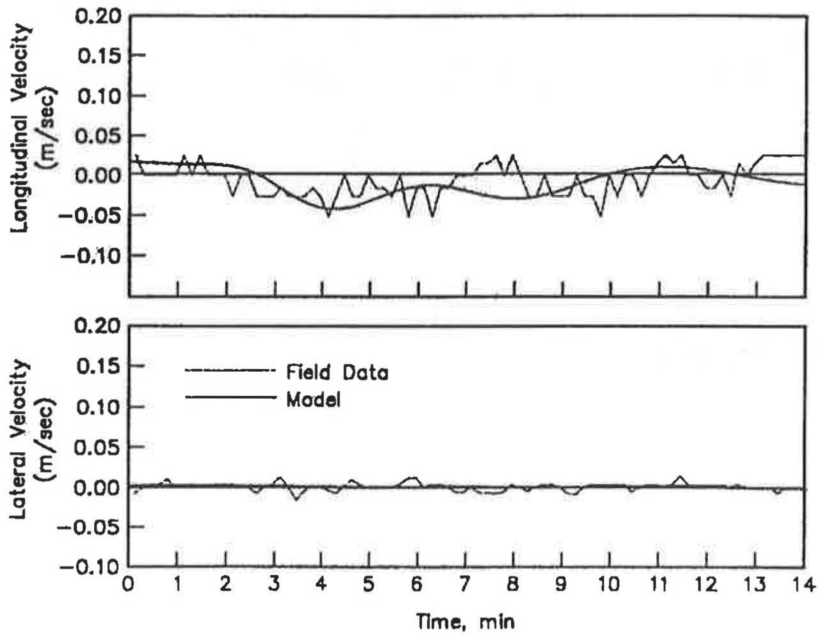

(b)

FIGURE 7 Velocities in Pool 8, Mississippi River: (a) vessel-generated currents at R2; (b) vessel-generated currents at R6 ***(continued on next page)***

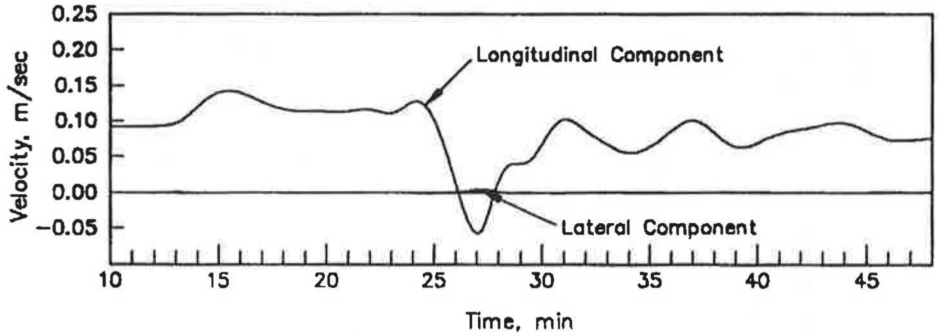

(c)

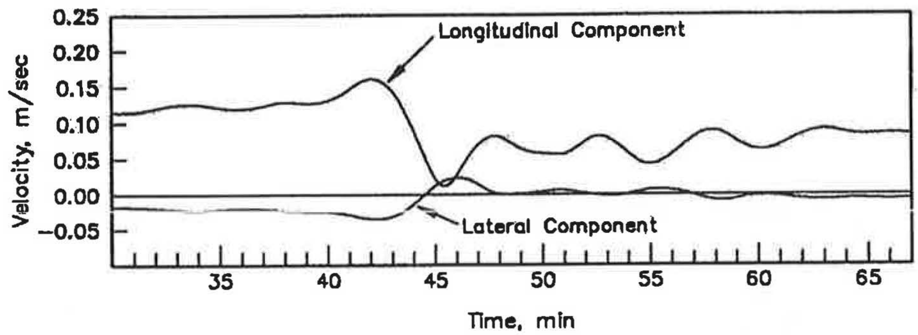

(d)

FIGURE 7 ***(continued)*** **Velocities in Pool 8, Mississippi River: (c) total velocity at P7; (d) total velocity at P15.**

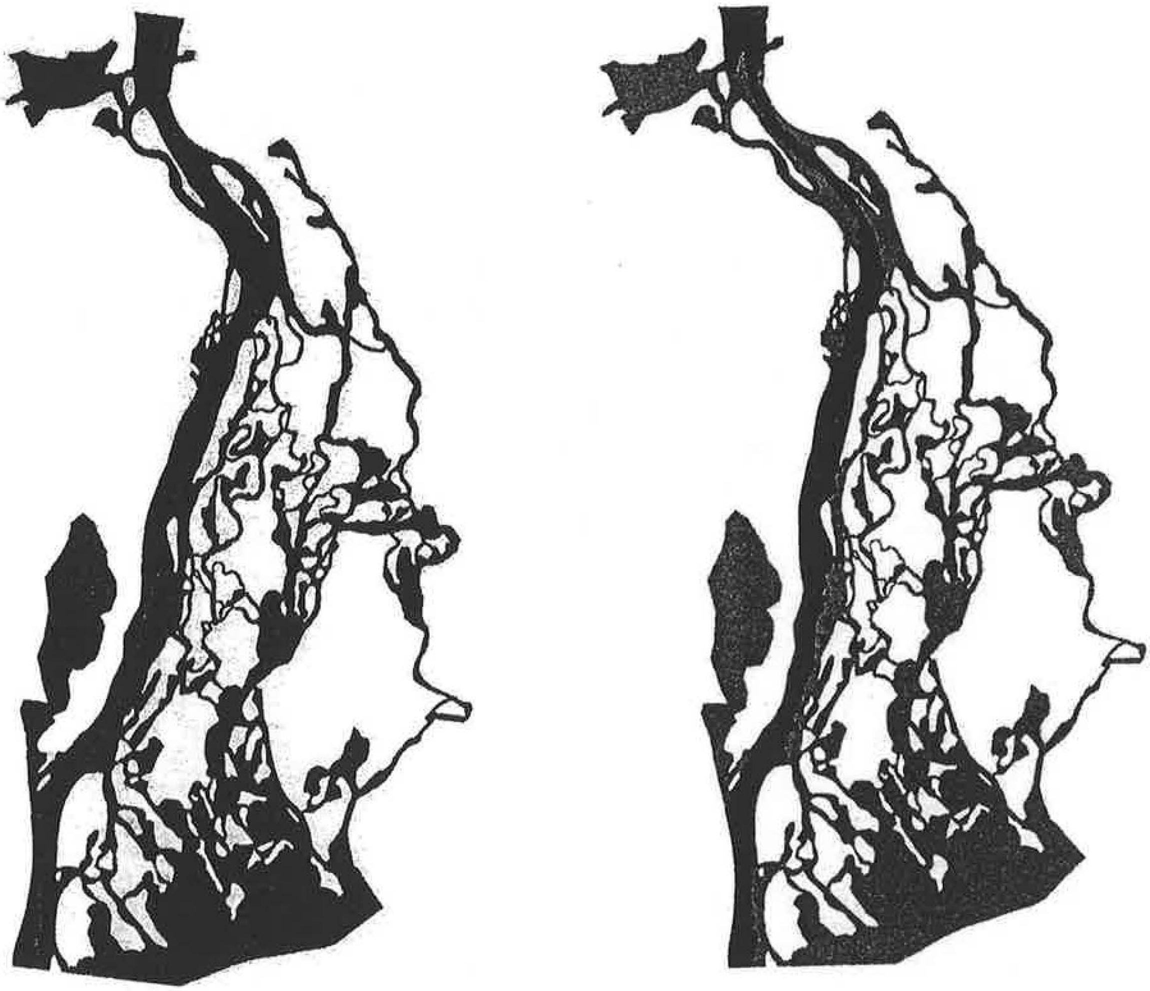

(a) **(b)**

FIGURE 8 Model results in Pool 8, Mississippi River: (a) Vessel-generated drawdown, black indicates regions of greater than 0.1m drawdown; (b) Vessel-generated currents, black indicates regions of greater than 0.2 m/sec velocity.